Engineering Computations

Degenerate-scale problem of the boundary integral equation method/boundary element method for the bending plate analysis

Jeng-Tzong Chen, Shyh-Rong Kuo, Yu-Lung Chang, Shing-Kai Kao,

Degenerate-scale problem of the boundary integral equation method/boundary element method for the bending plate analysis

Jeng-Tzong Chen
Department of Harbor and River Engineering, National Taiwan Ocean University, Keelung, Taiwan and Department of Mechanical and Mechatronic Engineering, National Taiwan Ocean University, Keelung, Taiwan, and

Shyh-Rong Kuo, Yu-Lung Chang and Shing-Kai Kao
Department of Harbor and River Engineering, National Taiwan Ocean University, Keelung, Taiwan

Received 1 June 2016
Revised 6 September 2016
27 October 2016
30 October 2016
Accepted 31 October 2016

Abstract

Purpose – The purpose of this paper is to detect the degenerate scale of a 2D bending plate analytically and numerically.

Design/methodology/approach – To avoid the time-consuming scheme, the influence matrix of the boundary element method (BEM) is reformulated to an eigenproblem of the 4 by 4 matrix by using the scaling transform instead of the direct-searching scheme to find degenerate scales. Analytical degenerate scales are derived from the boundary integral equation (BIE) by using the degenerate kernel only for the circular case. Numerical results of the direct-searching scheme and the eigen system for the arbitrary shape are also considered.

Findings – Results using three methods, namely, analytical derivation, the direct-searching scheme and the 4 by 4 eigen system, are also given for the circular case and arbitrary shapes. Finally, addition of a constant for the kernel function makes original eigenvalues (2 real roots and 2 complex roots) of the 4 by 4 matrix to be all real. This indicates that a degenerate scale depends on the kernel function.

Originality/value – The analytical derivation for the degenerate scale of a 2D bending plate in the BIE is first studied by using the degenerate kernel. Through the reformed eigenproblem of a 4 by 4 matrix, the numerical solution for the plate of an arbitrary shape can be used in the plate analysis using the BEM.

Keywords Boundary integral equation, Arbitrary shapes, Circular plate, Degenerate kernel, Degenerate scales, Eigenproblem of the 4 by 4 matrix

Paper type Research paper

1. Introduction

Boundary element method (BEM) was developed by discretizing the boundary integral equation (BIE), and has been first applied for the elasticity problem by Rizzo in 1967. The BEM has been also utilized to solve many problems, *e.g.,* potential problem (He *et al.*, 1996), Navier equation for elasticity (Zhou *et al.*, 1999; Chen and Lin, 2010; Chen and Wang, 2015), Helmholtz equation (Chen *et al.*, 2003a) and biharmonic equation (Mitra and Das, 1988;

Financial support from the Ministry of Science and Technology under Grant No. MOST 103-2221-E-019-012-MY3 and MOST 104-2221-E-019-007-MY3 for National Taiwan Ocean University is gratefully acknowledged.

Engineering Computations
Vol. 34 No. 5, 2017
pp. 1527-1550

0264-4401
DOI 10.1108/EC-06-2016-0187

Constanda, 1997; He, 2000). To reduce the preprocessing time of model creation, the BEM is more efficient than the domain-type method, *e.g.,* finite element method (FEM) and finite difference method. Until now, there are many research studies about the BEM to deal with numerical issues and about the improvement for the BEM.

Degenerate scale is one pitfall in the BEM. From a mathematical or numerical point of view, problems of the degenerate scale exist in the boundary integral equation method (BIEM)/BEM. There are several terminologies for the degenerate scale, *e.g.,* the critical value (Yan and Sloan, 1988), the transfinite diameter (Yan and Sloan, 1988; Christiansen, 2001), the Gamma contour and the unit logarithmic capacity (Hille, 1962; Hayes and Kellner, 1972; Constanda, 1993; Dijkstra and Mattheij, 2007; Corfdir and Bonnet, 2013; Kuo *et al.*, 2013a, 2013b) in the modern potential theory. In addition to the degenerate scale of a circle (Petrovsky, 1954; Vodička and Mantič, 2004; Vodička and Mantič, 2008; Lee *et al.*, 2013), Chen *et al.* had studied the degenerate scales of an elliptic case (Chen *et al.*, 2012), a regular *N*-gon (Kuo *et al.*, 2013a, 2013b) and a semi-circular disc (Chen *et al.*, 2015) by using the unit logarithmic capacity through the complex variables and the BEM. In the BEM, the degenerate scale stems from the rank deficiency problems due to the fundamental solution ln(r) for the 2D Laplace equation subject to the Dirichlet boundary condition (Chen *et al.*, 2001, 2002, 2003b, 2005a; Han *et al.*, 2015). Degenerate scales of the plane elasticity were studied by Chen *et al.* (2009a, 2009b, 2009c). Corfdir and Bonnet (2016) used the complex variable methods to find the exact degenerate scales in plane elasticity. To deal with degenerate scales, there are several regularized approaches, *e.g.,* the method of adding rigid body mode (Chen *et al.*, 2005a, 2014), rank promotion by adding the boundary flux equilibrium (Chen *et al.*, 2014), hypersingular integral formulation (Chen *et al.*, 2014), CHEFF method (Chen *et al.*, 2002, 2005a; Chen *et al.*, 2014), the Fichera's method (Chen *et al.*, 2014) and the self-regularization method (Chen *et al.*, 2017a). According to the Fredholm alternative theorem and the bordered matrix, the slack variable in the Fichera's method was used to distinguish two cases of the non-uniqueness of the solution, the rigid body mode in physics and the degenerate scale in the BEM (Chen *et al.*, 2014, 2017a).

Regarding the mathematical model of the 2D biharmonic equation, there are many engineering applications, such as plate and Stokes' flow problems. The Kirchhoff thin plate is a classic problem for the biharmonic equation. Yu (1982, 1983, 1993, 2002) used the canonical integral equation and the natural BEM to solve the boundary value problem of the biharmonic equation. Chen and Zhou (1992) pointed out the merit of using the BEM to deal with the biharmonic equation. The biharmonic equation of the plate problem can be also computed by using the FEM, provided that either the higher-order conforming elements are used or some patch tests are utilized to check with lower-order nonconforming elements. It may lead to a heavy loading to the computation while extra work is added to the isoparametric transformation for the curved boundary. In fact, the BEM is more efficient than the FEM in handling the higher-order partial different equation. To deal with the biharmonic equation, the BIEs for the plate problems were acquired from the Rayleigh–Green identity (Chen *et al.*, 2006a, 2005b) for the BEM. Some pioneering works were done by Jaswon *et al.* (1967) and Jawson and Maiti (1968), who introduced the kernel functions into the BIE to deal with the plate problem. Then, Stern (1979) proposed the application of the BEM for the plate problem. For thick Reissner plates, Fadhil and El-Zafrany (1994) derived an alternative BEM formulation resting on a one- or two-parameter elastic foundation. As the method of the fundamental solutions (MFS) is equivalent to the indirect BEM, Tsiatas (2009) derived a new Kirchhoff plate model based on a modified couple stress theory and numerically implemented by using the MFS. Manolis *et al.* (2003) used Radon transform to derive fundamental solutions for the non-homogeneous 2D biharmonic equation in the half-space. Similar to the Laplace equation,

degenerate scales for the 2D biharmonic equation results from the fundamental solution $r^2\ln(r)$. Chen *et al.* (2006a, 2005b, 2007a, 2007b, 2009d) had studied the biharmonic equation by using the null-field BIEM or Green's function. Costabel and Dauge (1996) proposed the theory that a 4 by 4 matrix of the eigenproblem was derived for the biharmonic equation. However, the numerical implementation for the arbitrary domain was not mentioned. Only two-trials technique (2 by 2 eigenvalue problem) was used to search the degenerate scales in plane elasticity in the work by Chen *et al.* (2017b). Based on the similar idea, we may extend to find the degenerate scales of the biharmonic equation.

In this paper, the biharmonic equation is revisited by using the indirect BIEs and the indirect BEM. The concept of the separation of source and field points can be applied in transforming the original problem to the eigenproblem in the subspace by using the scaling transform. The validity of the proposed method is verified by several numerical cases.

2. Problem statement

The governing equation for a two-dimensional Kirchhoff plate under the distributed load $w(\mathbf{x})$ is written as follows:

$$\nabla^4 u^*(\mathbf{x}) = \frac{w(\mathbf{x})}{D}, \qquad \mathbf{x} \in \Omega \tag{1}$$

where $u^*(\mathbf{x})$ is the lateral displacement, Ω is the domain of the thin plate and the flexural rigidity D can be expressed as:

$$D = \frac{Eh^3}{12(1-\nu^2)} \tag{2}$$

where E is Young's modulus, h is the thickness of the plate and v is the Poisson ratio. The simple situation of the clamped case is considered as:

$$u^*(\mathbf{x}) = 0, \qquad \theta^*(\mathbf{x}) = 0, \qquad \mathbf{x} \in B \tag{3}$$

where $\theta^*(\mathbf{x})$ is the slope and B is the boundary of the domain. The total solution $u^*(\mathbf{x})$ can be superimposed by a complementary solution $u(\mathbf{x})$ and a particular solution due to $w^*(\mathbf{x})$. Therefore, the lateral loading of $u(\mathbf{x})$ is zero. We have:

$$\nabla^4 u(\mathbf{x}) = 0, \qquad \mathbf{x} \in \Omega \tag{4}$$

and the essential boundary conditions:

$$u(\mathbf{x}) = u_b(\mathbf{x}), \qquad \frac{\partial u(\mathbf{x})}{\partial n_{\mathbf{x}}} = \theta(\mathbf{x}) = \theta_b(\mathbf{x}), \qquad \mathbf{x} \in B \tag{5}$$

where $u(\mathbf{x})$ is the displacement, $\partial/\partial n_{\mathbf{x}}$ is the normal derivative with respect to the field point $\mathbf{x}$ and $\theta(\mathbf{x})$ is the slope.

2.1 Indirect boundary integral equations

Indirect BIEM stems from the physical concept of superposition. The integral representation for the solution satisfies the governing equation. The unknown boundary density can be

determined by matching the boundary conditions. For simplicity, single- and double-layer potentials (Chen and Zhou, 1992) are chosen for the biharmonic equation as follows:

$$u(\mathbf{x}) = \int_B U(\mathbf{x},\mathbf{s})\Phi(\mathbf{s})dB(\mathbf{s}) + \int_B \Theta(\mathbf{x},\mathbf{s})\Psi(\mathbf{s})dB(\mathbf{s}),\ \mathbf{x}\in\Omega \tag{6}$$

where $\Phi(\mathbf{s})$ and $\Psi(\mathbf{s})$ are boundary densities, respectively. The normal derivative with respect to equation (6) can be expressed as:

$$\theta(\mathbf{x}) = \int_B U_\theta(\mathbf{x},\mathbf{s})\Phi(\mathbf{s})dB(\mathbf{s}) + \int_B \Theta_\theta(\mathbf{x},\mathbf{s})\Psi(\mathbf{s})dB(\mathbf{s}),\ \mathbf{x}\in\Omega \tag{7}$$

For a domain point $\mathbf{x}\in\Omega$, the selection for the normal vector by $n_{\mathbf{x}}^d$ can be assumed in an arbitrary direction, where $n_{\mathbf{x}}^d$ is the normal vector of the domain point $\mathbf{x}\in\Omega$. Therefore, the selection for the normal vector n_x depends on the user's choice. For example, we obtain $\partial u(\mathbf{x})/\partial x$ by choosing $n_{\mathbf{x}}^d = (1, 0)$, while we have $\partial u(\mathbf{x})/\partial x$ by choosing $n_{\mathbf{x}}^d = (0, 1)$. In addition, when the domain point $\mathbf{x}\in\Omega$ is approaching a boundary point $\mathbf{x}_b\in$ B, the relevant vector $n_{\mathbf{x}}^d$ must approach a definite normal vector $n_{\mathbf{x}}^b$ assumed at the boundary point $\mathbf{x}_b\in$ B. The relationship among the four kernel functions ($U(\mathbf{x}, \mathbf{s})$, $\Theta(\mathbf{x}, \mathbf{s})$, $U_\theta(\mathbf{x}, \mathbf{s})$ and $\Theta_\theta(\mathbf{x}, \mathbf{s})$) used in indirect BIEs is introduced by using the fundamental solutions for the biharmonic equation, and the degenerate form of four kernels by separating the field point $\mathbf{x} = (\rho, \phi)$ and the source point $\mathbf{s} = (R, \theta)$ can be expressed in the polar coordinates as:

$$U(\mathbf{x},\mathbf{s}) = r^2\ln R = \begin{cases} U^I(\mathbf{x},\mathbf{s}) = \rho^2(1+\ln R) + R^2\ln R - \left[R\rho(1+2\ln R) + \dfrac{1}{2}\dfrac{\rho^3}{R}\right]\cos(\theta-\phi) \\ \quad -\displaystyle\sum_{m=2}^{\infty}\left[\frac{1}{m(m+1)}\frac{\rho^{m+2}}{R^m} - \frac{1}{m(m-1)}\frac{\rho^m}{R^{m-2}}\right]\cos[m(\theta-\phi)], \quad R\geq\rho, \\ U^E(\mathbf{x},\mathbf{s}) = R^2(1+\ln\rho) + \rho^2\ln\rho - \left[\rho R(1+2\ln\rho) + \dfrac{1}{2}\dfrac{R^3}{\rho}\right]\cos(\theta-\phi) \\ \quad -\displaystyle\sum_{m=2}^{\infty}\left[\frac{1}{m(m+1)}\frac{R^{m+2}}{\rho^m} - \frac{1}{m(m-1)}\frac{R^m}{\rho^{m-2}}\right]\cos[m(\theta-\phi)], \quad \rho > R \end{cases} \tag{8}$$

$$\Theta(\mathbf{x},\mathbf{s}) = \begin{cases} \Theta^I(\mathbf{x},\mathbf{s}) = \dfrac{\rho^2}{R} + R(2\ln R+1) - \left[\rho(3+2\ln R) - \dfrac{1}{2}\dfrac{\rho^3}{R^2}\right]\cos(\theta-\phi) \\ \quad +\displaystyle\sum_{m=2}^{\infty}\left[\frac{1}{(m+1)}\frac{\rho^{m+2}}{R^{m+1}} - \frac{m-2}{m(m-1)}\frac{\rho^m}{R^{m-1}}\right]\cos[m(\theta-\phi)], \quad R\geq\rho, \\ \Theta^E(\mathbf{x},\mathbf{s}) = 2R(1+\ln\rho) - \left[\rho(1+2\ln\rho) + \dfrac{3}{2}\dfrac{R^2}{\rho}\right]\cos(\theta-\phi) \\ \quad -\displaystyle\sum_{m=2}^{\infty}\left[\frac{m+2}{m(m+1)}\frac{R^{m+1}}{\rho^m} - \frac{1}{(m-1)}\frac{R^{m-1}}{\rho^{m-2}}\right]\cos[m(\theta-\phi)], \quad \rho > R \end{cases} \tag{9}$$

$$U_\theta(\mathbf{x},\mathbf{s})=\begin{cases} U_\theta^I(\mathbf{x},\mathbf{s})=2\rho(1+\ln R)-\left[R(1+2\ln R)+\frac{3}{2}\frac{\rho^2}{R}\right]\cos(\theta-\phi) \\ -\sum_{m=2}^{\infty}\left[\frac{m+2}{m(m+1)}\frac{\rho^{m+1}}{R^m}-\frac{1}{(m-1)}\frac{\rho^{m-1}}{R^{m-2}}\right]\cos[m(\theta-\phi)], \quad R\geq\rho, \\ U_\theta^E(\mathbf{x},\mathbf{s})=\frac{R^2}{\rho}+\rho(2\ln\rho+1)-\left[R(3+2\ln\rho)-\frac{1}{2}\frac{R^3}{\rho^2}\right]\cos(\theta-\phi) \\ +\sum_{m=2}^{\infty}\left[\frac{1}{m+1}\frac{R^{m+2}}{\rho^{m+1}}-\frac{m-2}{m(m-1)}\frac{R^m}{\rho^{m-1}}\right]\cos[m(\theta-\phi)], \quad \rho>R \end{cases} \tag{10}$$

and

$$\Theta_\theta(\mathbf{x},\mathbf{s})=\begin{cases} \Theta_\theta^I(\mathbf{x},\mathbf{s})=\frac{2\rho}{R}-\left[(3+2\ln R)-\frac{3}{2}\frac{\rho^2}{R^2}\right]\cos(\theta-\phi) \\ +\sum_{m=2}^{\infty}\left[\frac{m+2}{m+1}\frac{\rho^{m+1}}{R^{m+1}}-\frac{m-2}{m-1}\frac{\rho^{m-1}}{R^{m-1}}\right]\cos[m(\theta-\phi)], \quad R\geq\rho, \\ \Theta_\theta^E(\mathbf{x},\mathbf{s})=\frac{2R}{\rho}-\left[(3+2\ln\rho)-\frac{3}{2}\frac{R^2}{\rho^2}\right]\cos(\theta-\phi) \\ +\sum_{m=2}^{\infty}\left[\frac{m+2}{m+1}\frac{R^{m+1}}{\rho^{m+1}}-\frac{m-2}{m-1}\frac{R^{m-1}}{\rho^{m-1}}\right]\cos[m(\theta-\phi)], \quad \rho>R \end{cases} \tag{11}$$

The superscripts "I" and "E" denote the interior and exterior cases, respectively. The contour plots of $U(\mathbf{x}, \mathbf{s})$ for the degenerate kernel in polar coordinates and closed-form fundamental solution are shown in Figure 1. The boundary densities in equations (6) and (7) along a circular boundary are expressed in terms of Fourier series as follows:

$$\Phi(\mathbf{s}) = a_0 + \sum_{n=1}^{\infty}(a_n\cos n\theta + b_n\sin n\theta), \quad \mathbf{s}\in B \tag{12}$$

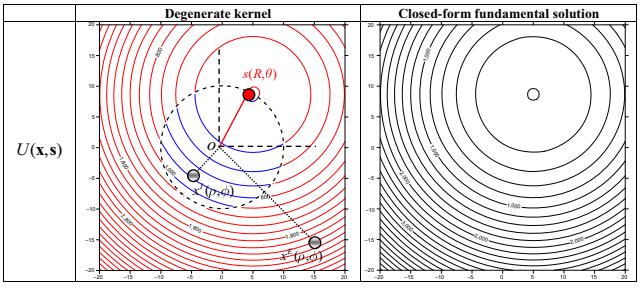

Notes: s located at R = 10.0, $\theta = \frac{\pi}{3}$

Figure 1.
Sketch of contour plots for the degenerate kernel in polar coordinates and closed-form fundamental solution

$$\Psi(\mathbf{s}) = c_0 + \sum_{n=1}^{\infty}(c_n \cos n\theta + d_n \sin n\theta), \qquad \mathbf{s} \in B \tag{13}$$

where a_O, a_n, b_n, c_0, c_n and d_n are the Fourier coefficients.

By introducing degenerate kernels for the interior problem and Fourier expressions for the boundary densities from equations (8)-(13) and integrating on the boundary, the parts of equations (6) and (7) can be reformulated as:

$$\int_B U(\mathbf{x},\mathbf{s})\Phi(\mathbf{s})dB(\mathbf{s}) = 2\pi(1+2\ln R_0)R_0^3 a_0 - \pi\left(\frac{3}{2}+2\ln R_0\right)a_1 R_0^3 \cos\phi - \pi\left(\frac{3}{2}+\ln R_0\right)b_1 R_0^3 \sin\phi$$
$$+\sum_{m=2}^{\infty}\frac{2\pi}{m(m+1)(m-1)}a_m R_0^3 \cos m\phi + \sum_{m=2}^{\infty}\frac{2\pi}{m(m+1)(m-1)}b_m R_0^3 \sin m\phi \tag{14}$$

$$\int_B \Theta(\mathbf{x},\mathbf{s})\Psi(\mathbf{s})dB(\mathbf{s}) = 4\pi(1+\ln R_0)c_0 R_0^2 - \pi\left(\frac{5}{2}+2\ln R_0\right)c_1 R_0^2 \cos\phi - \pi\left(\frac{5}{2}+2\ln R_0\right)d_1 R_0^2 \sin\phi$$
$$+\sum_{m=2}^{\infty}\frac{2\pi}{m(m+1)(m-2)}c_m R_0^2 \cos m\phi + \sum_{m=2}^{\infty}\frac{2\pi}{m(m+1)(m-2)}d_m R_0^2 \sin m\phi \tag{15}$$

$$\int_B U_\theta(\mathbf{x},\mathbf{s})\Phi(\mathbf{s})dB(\mathbf{s}) = 4\pi(1+\ln R_0)a_0 R_0^2 - \pi\left(\frac{5}{2}+2\ln R_0\right)a_1 R_0^2 \cos\phi - \pi\left(\frac{5}{2}+2\ln R_0\right)b_1 R_0^2 \sin\phi$$
$$+\sum_{m=2}^{\infty}\frac{2\pi}{m(m+1)(m-1)}a_m R_0^2 \cos m\phi + \sum_{m=2}^{\infty}\frac{2\pi}{m(m+1)(m-1)}b_m R_0^2 \sin m\phi \tag{16}$$

and:

$$\int_B \Theta_\theta(\mathbf{x},\mathbf{s})\Psi(\mathbf{s})dB(\mathbf{s}) = 4\pi R_0 c_0 - \pi\left(\frac{3}{2}+2\ln R_0\right)c_1 R_0 \cos\phi - \pi\left(\frac{3}{2}+2\ln R_0\right)d_1 R_0 \sin\phi$$
$$+\sum_{m=2}^{\infty}\frac{2m\pi}{(m+1)(m-1)}c_m R_0 \cos m\phi + \sum_{m=2}^{\infty}\frac{2m\pi}{(m+1)(m-1)}d_m R_0 \sin m\phi \tag{17}$$

where R_0 is the radius of the circular domain.

The displacement $u(\mathbf{x})$ and the slope $\theta(\mathbf{x})$ in equation (5) can be expressed in terms of Fourier series as follows:

$$u(\mathbf{x}) = u_b(\mathbf{x}) = e_0 + \sum_{n=1}^{\infty}(e_n \cos n\theta + f_n \sin n\theta), \qquad \mathbf{x} \in B \tag{18}$$

$$\theta(\mathbf{x}) = \theta_b(\mathbf{x}) = g_0 + \sum_{n=1}^{\infty}(g_n \cos n\theta + h_n \sin n\theta), \qquad \mathbf{x} \in B \tag{19}$$

Where e_0, e_n, f_n, g_0, g_n and h_n are the Fourier coefficients. By comparing the coefficient and taking the constant term, the term related to cos θ and the term related to sin θ, the coefficient can be determined by:

$$\begin{bmatrix} 2\pi(1+2\ln R_0)R_0^3 & 4\pi(1+\ln R_0)R_0^2 & 0 & 0 & 0 & 0 \\ 4\pi(1+\ln R_0)R_0^2 & 4\pi R_0 & 0 & 0 & 0 & 0 \\ 0 & 0 & -\pi\left(\frac{3}{2}+2\ln R_0\right)R_0^3 & -\pi\left(\frac{5}{2}+2\ln R_0\right)R_0^2 & 0 & 0 \\ 0 & 0 & -\pi\left(\frac{5}{2}+2\ln R_0\right)R_0^2 & -\pi\left(\frac{3}{2}+2\ln R_0\right)R_0 & 0 & 0 \\ 0 & 0 & 0 & 0 & -\pi\left(\frac{3}{2}+2\ln R_0\right)R_0^3 & -\pi\left(\frac{5}{2}+2\ln R_0\right)R_0^2 \\ 0 & 0 & 0 & 0 & -\pi\left(\frac{5}{2}+2\ln R_0\right)R_0^2 & -\pi\left(\frac{3}{2}+2\ln R_0\right)R_0 \end{bmatrix} \begin{Bmatrix} a_0 \\ c_0 \\ a_1 \\ c_1 \\ b_1 \\ d_1 \end{Bmatrix} = \begin{Bmatrix} e_0 \\ g_0 \\ e_1 \\ f_1 \\ g_1 \\ h_1 \end{Bmatrix} \tag{20}$$

To clearly study the degenerate scale, two conditions, $u(\mathbf{x}) = 0$ and $\theta(\mathbf{x}) = 0$, $\mathbf{x} \in B$, are adopted. Therefore, the Fourier coefficients of boundary conditions, e_0, g_0, e_1, f_1, g_1 and h_1, are zero in equation (20). In case of a degenerate scale, there exists a non-trivial boundary density while the homogeneous essential boundary condition is given. If a size of the circular boundary is the degenerate scale, the influence matrix in the left-hand side of equation (20) is singular. In other words, to solve the coefficients of equation (20), a_0, c_0, a_1, c_1, b_1 and d_1, the determinant of the submatrix is equal to zero while a degenerate scale occurs. The determinant of the submatrix for unknown coefficients, a_0 and c_0, is zero as:

$$R_d^4\left[(1+2\ln R_d) - 2(1+\ln R_d)^2\right] = 0 \tag{21}$$

and the degenerate scale $R_d = -\frac{1+i}{2}$. As the radius R_d is real, no real R_d can be found to satisfy equation (21). The matrices for solving unknown coefficients, a_1, c_1, b_1 and d_1, are the same. Similarly, we can determine the degenerate scale by using the zero determinant:

$$R_d^4\left[\left(\frac{3}{2}+2\ln R_d\right)^2 - \left(\frac{5}{2}+2\ln R_d\right)^2\right] = 0 \tag{22}$$

and find the degenerate scale $R_d = e^{-1}$(a double root). It means that coefficients of the constant term can be determined even while the degenerate scale occurs ($R_d = e^{-1}$), but the coefficients of the term related to cos θ and sin θ cannot be determined. The analytical degenerate scale of the biharmonic equation ($R_d = e^{-1}$) was also obtained through the Fourier expansion by Chen and Zhou (1992), although the degenerate kernel for the fundamental solution was not used in their book.

2.2 Direct-searching scheme to find the degenerate scale

By using the boundary element scheme, equations (6) and (7) yield a linear algebraic system:

$$[\mathrm{A}]\{x\} = \{b_\mathrm{T}\} \tag{23}$$

where $[\mathbf{A}]$ is the influence matrix from:

$$[\mathbf{A}]_{2N\times 2N} = \begin{bmatrix} [\mathbf{U}]_{N\times N} & [\mathbf{\Theta}]_{N\times N} \\ [\mathbf{U}_\theta]_{N\times N} & [\mathbf{\Theta}_\theta]_{N\times N} \end{bmatrix} \tag{24}$$

in which N is the number of boundary elements, $\{b_T\}$ is the given boundary condition and $\{x\}$ is the unknown vector constructed by boundary densities, $\Phi(\mathbf{s})$ and $\Psi(\mathbf{s})$. By changing the size, the influence matrix $\mathbf{A}$ may be singular (the minimum singular value is zero) and the boundary densities could not be determined while this size is a degenerate scale. Although the direct-searching scheme to find the minimum singular value by using the singular value decomposition (SVD) (Chen *et al.*, 2005b) can straightforwardly find the degenerate scale step by step, it is not efficient due to many trials.

2.3 Reduction to a 4 by 4 eigen system by using the scaling transform

The fundamental solution for the biharmonic equation can be obtained as:

$$U(\mathbf{x},\mathbf{s}) = r^2 \ln R \tag{25}$$

where $r = |\mathbf{x}-\mathbf{s}| = |\rho e^{i\phi} - \mathrm{R}e^{i\theta}|$ is the distance between the source point $\mathbf{s}$ and field point $\mathbf{x}$ in terms of polar coordinates.

When the distance r is extended to pr after scaling ($\mathbf{x} \to p\mathbf{x}$, $\mathrm{s} \to p\mathbf{s}$) as shown in Figure 2, the fundamental solution in equation (25) can be changed to:

$$U^p(\mathbf{x},\mathbf{s}) = \frac{1}{2}(pr)^2 \ln(pr)^2 = p^2\left(\frac{1}{2}r^2 \ln r^2\right) + p^2(\ln p)(r^2) \tag{26}$$

Then, the scaling influence matrix corresponding to the new size extends to:

$$[\mathbf{U}^p] = p^2[\mathbf{U}] + p^2 \ln p[\mathrm{U}^{ps}] \tag{27}$$

where $[\mathbf{U}^{ps}]$ is obtained due to scaling of equation (26), and the other influence matrices can be similarly represented as:

$$[\mathbf{\Theta}^p] = p[\mathbf{\Theta}] + p \ln p[\mathbf{\Theta}^{ps}] \tag{28}$$

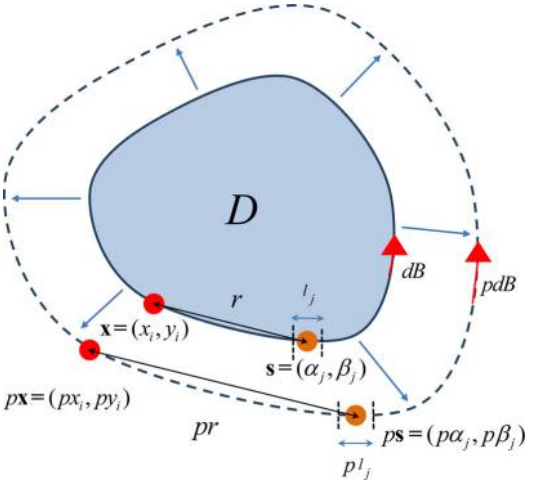

Figure 2.
The field point and the source point after the scaling transform

$$\left[\mathbf{U}_\theta^p\right] = p\left[\mathbf{U}_\theta\right] + p\ln p\left[\mathbf{U}_\theta^{ps}\right] \tag{29}$$

$$\left[\mathbf{\Theta}_\theta^p\right] = \left[\mathbf{\Theta}_\theta\right] + \ln p\left[\mathbf{\Theta}_\theta^{ps}\right] \tag{30}$$

where $[\mathbf{U}]$, $[\mathbf{\Theta}]$, $[\mathbf{U}_\theta]$ and $[\mathbf{\Theta_0}]$ are the original influence matrices and the four extra matrices, $[\mathbf{U}^{ps}]$, $[\mathbf{\Theta}^{ps}]$, $\left[\mathbf{U}_\theta^{ps}\right]$ and $\left[\mathbf{\Theta}_\theta^{ps}\right]$, can be represented as:

$$\begin{aligned}(U^{ps})_{ij} &= \int_{l_j} r_{ij}^2 dB(\mathbf{s}) \approx \left((x_i-\alpha_j)^2 + (y_i-\beta_j)^2\right) l_j \\ &= \left[1,\, x_i,\, y_i,\, (x_i^2+y_i^2)\right]\cdot\left[\left(\alpha_j^2+\beta_j^2\right)l_j,\, (-2\alpha_j)l_j,\, (-2\beta_j)l_j,\, (1)l_j\right] \\ &= \phi(x_i, y_i)\psi^T(\alpha_j, \beta_j)\end{aligned} \tag{31}$$

$$\begin{aligned}(\theta^{ps})_{ij} &= \int_{l_j} \frac{\partial}{\partial n_{\mathbf{s}_i}} r_{ij}^2 dB(\mathbf{s}) \approx \frac{\partial}{\partial n_{\mathbf{s}_i}}\left((x_i-\alpha_j)^2 + (y_i-\beta_j)^2\right) l_j \\ &= \left[1,\, x_i,\, y_i,\, (x_i^2+y_i^2)\right]\cdot\left[2(\alpha_j n_{\alpha j}+\beta_j n_{\beta j})l_j,\, (-2n_{\alpha j})l_j,\, (-2_{\beta j})l_j,\, 0\right] \\ &= \phi(x_i, y_i)\psi_n^T(\alpha_j, \beta_j)\end{aligned} \tag{32}$$

$$\begin{aligned}\left(U_\theta^{ps}\right)_{ij} &= \int_{l_j} \frac{\partial}{\partial n_{\mathbf{x}_i}} r_{ij}^2 dB(\mathbf{s}) \approx \frac{\partial}{\partial n_{\mathbf{x}_i}}\left((x_i-\alpha_j)^2 + (y_i-\beta_j)^2\right) l_j \\ &= \left(2(x_i-\alpha_j)(n_{xi}) + 2(y_i-\beta_j)n_{yi}\right)l_j \\ &= \left[0,\, n_{xi},\, n_{yi},\, 2(x_i n_{xi}+y_i n_{yi})\right]\cdot\left[\left(\alpha_j^2+\beta_j^2\right)l_j,\, (-2\alpha_j)l_j,\, (-2\beta_j)l_j,\, (1)l_j\right] \\ &= \phi_n(x_i, y_i)\psi^T(\alpha_j, \beta_j)\end{aligned} \tag{33}$$

$$\begin{aligned}\left(\theta_\theta^{ps}\right)_{ij} &= \int_{l_j} \frac{\partial}{\partial n_{\mathbf{x}_i} n_{\mathbf{s}_j}} r_{ij}^2 dB(\mathbf{s}) \approx \frac{\partial}{\partial n_{\mathbf{x}_i} n_{\mathbf{s}_j}}\left((x_i-\alpha_j)^2 + (y_i-\beta_j)^2\right) l_j \\ &= \left[0,\, n_{xi},\, n_{yi},\, 2(x_i n_{xi}+y_i n_{yi})\right]\cdot\left[2(\alpha_j n_{\alpha j}+\beta_j n_{\beta j})l_j,\, (-2n_{\alpha j})l_j,\, (-2n_{\beta j})l_j,\, 0\right] \\ &= \phi_n(x_i, y_i)\psi_n^T(\alpha_j, \beta_j)\end{aligned} \tag{34}$$

respectively, where l_j is the length of the boundary element, the source point $\mathbf{s} = (\alpha_j, \beta_j)$ and the field point $\mathbf{x} = (x_i, y_i)$ are shown in Figure 2. It is found that the former middle bracket is the field-point (x_i, y_i) dependent and the latter middle bracket is the source-point (α_j, β_j) dependent.

The influence matrix can be represented as:

$$[\mathbf{A}^{p}]_{2N\times 2N} = \begin{bmatrix} [\mathbf{U}^{p}]_{N\times N} & [\mathbf{\Theta}^{p}]_{N\times N} \\ \left[\mathbf{U}_{\theta}^{p}\right]_{N\times N} & \left[\mathbf{\Theta}_{\theta}^{p}\right]_{N\times N} \end{bmatrix} = \begin{bmatrix} p^{2}[\mathbf{U}] & p[\mathbf{\Theta}] \\ p[\mathbf{U}_{\theta}] & [\mathbf{\Theta}_{\theta}] \end{bmatrix} + \ln p \begin{bmatrix} p^{2}[\mathbf{U}^{ps}] & p[\mathbf{\Theta}^{ps}] \\ p\left[\mathbf{U}_{\theta}^{ps}\right] & \left[\mathbf{\Theta}_{\theta}^{ps}\right] \end{bmatrix} \tag{35}$$

If we transform the matrix $[\mathbf{A}^{p}]$ to:

$$\begin{bmatrix} \frac{1}{p}[\mathbf{I}]_{N\times N} & 0 \\ 0 & [\mathbf{I}]_{N\times N} \end{bmatrix} [\mathrm{A}^{p}] \begin{bmatrix} \frac{1}{p}[\mathbf{I}]_{N\times N} & 0 \\ 0 & [\mathbf{I}]_{N\times N} \end{bmatrix} = \left[\mathrm{A}^{pt}\right] \tag{36}$$

the transformed matrix $[\mathbf{A}^{pt}]$ can be represented as:

$$\left[\mathrm{A}^{pt}\right] = \begin{bmatrix} [\mathbf{U}] & [\mathbf{\Theta}] \\ [\mathbf{U}_{\theta}] & [\mathbf{\Theta}_{\theta}] \end{bmatrix} + \ln p \begin{bmatrix} [\mathbf{U}^{ps}] & [\mathbf{\Theta}^{ps}] \\ \left[\mathbf{U}_{\theta}^{ps}\right] & \left[\mathbf{\Theta}_{\theta}^{ps}\right] \end{bmatrix} = [\mathrm{A}] + \ln p\left[\mathrm{A}^{s}\right] \tag{37}$$

The zero determinant of the transformed matrix $[\mathbf{A}^{pt}]$ results in the zero determinant of the matrix $[\mathbf{A}^{p}]$.

The extra matrix $[\mathbf{A}^{s}]$ is expressed as:

$$\begin{aligned} [\mathrm{A}^{s}] &= \begin{bmatrix} [\mathbf{U}^{ps}] & [\mathbf{\Theta}^{ps}] \\ \left[\mathbf{U}_{\theta}^{ps}\right] & \left[\mathbf{\Theta}_{\theta}^{ps}\right] \end{bmatrix} = \begin{bmatrix} \phi(x_i, y_i)\psi^{T}(\alpha_j, \beta_j) & \phi(x_i, y_i)\psi_{n}^{T}(\alpha_j, \beta_j) \\ \phi_{n}(x_i, y_i)\psi^{T}(\alpha_j, \beta_j) & \phi_{n}(x_i, y_i)\psi_{n}^{T}(\alpha_j, \beta_j) \end{bmatrix} \\ &= \begin{bmatrix} \phi \\ \phi_{n} \end{bmatrix} \left[\psi^{T}\ \psi_{n}^{T}\right] = [\ \mathbf{\Phi_x}][\ \mathbf{\Psi_s}]^{T} \end{aligned} \tag{38}$$

where $[\mathbf{\Phi_x}]$ and $[\mathbf{\Psi_s}]$ are:

$$\begin{aligned} [\ \mathbf{\Phi_x}] &= \begin{bmatrix} 1 & x_1 & y_1 & x_1^{2}+y_1^{2} \\ 1 & x_2 & y_2 & x_2^{2}+y_2^{2} \\ \vdots & \vdots & \vdots & \vdots \\ 1 & x_N & y_N & x_N^{2}+y_N^{2} \\ 0 & n_{x_1} & n_{y_1} & 2(x_1 n_{x_1}+y_1 n_{y_1}) \\ 0 & n_{x_2} & n_{y_2} & 2(x_2 n_{x_2}+y_2 n_{y_2}) \\ \vdots & \vdots & \vdots & \vdots \\ 0 & n_{x_N} & n_{x_N} & 2(x_N n_{x_N}+y_N n_{y_N}) \end{bmatrix}_{2N\times 4} \\ &= \begin{bmatrix} \{1\} & \{x_i\} & \{y_i\} & \{x_i^{2}+y_i^{2}\} \\ \{0\} & \{n_{xi}\} & \{n_{yi}\} & \{2(x_i n_{xi}+y_i n_{yi})\} \end{bmatrix}_{2N\times 4} \end{aligned} \tag{39}$$

and

$$
\begin{aligned}
[\,\boldsymbol{\Psi}_{\mathbf{s}}] &= \begin{bmatrix}
\left(\alpha_1^2+\beta_1^2\right)l_1 & -2\alpha_1 l_1 & -2\beta_1 l_1 & l_1 \\
\left(\alpha_2^2+\beta_2^2\right)l_2 & -2\alpha_2 l_2 & -2\beta_2 l_2 & l_2 \\
\vdots & \vdots & \vdots & \vdots \\
\left(\alpha_N^2+\beta_N^2\right)l_N & -2\alpha_N l_N & -2\beta_N l_N & l_N \\
2(\alpha_1 n_{\alpha_1}+\beta_1 n_{\beta_1})l_1 & -2n_{\alpha_1} l_1 & -2n_{\beta_1} l_1 & 0 \\
2(\alpha_2 n_{\alpha_2}+\beta_2 n_{\beta_2})l_2 & -2n_{\alpha_2} l_2 & -2n_{\beta_2} l_2 & 0 \\
\vdots & \vdots & \vdots & \vdots \\
2(\alpha_N n_{\alpha_N}+\beta_N n_{\beta_N})l_N & -2n_{\alpha_N} l_N & -2n_{\beta_N} l_N & 0
\end{bmatrix}_{2N\times 4} \\
&= \begin{bmatrix}
\left\{\left(\alpha_j^2+\beta_j^2\right)l_j\right\} & \{(-2\alpha_j)l_j\} & \{(-2\beta_j)l_j\} & \{(1)l_j\} \\
\{2(\alpha_j n_{\alpha j}+\beta_j n_{\beta j})l_j\} & \{(-2n_{\alpha j})l_j\} & \{(-2n_{\beta j})l_j\} & \{0\}
\end{bmatrix}_{2N\times 4}
\end{aligned}
\tag{40}
$$

consist of the field points (x_i, y_i) and the source points (α_j, β_j), respectively.

It means that the scaling matrix can be decomposed into two matrices as equation (38) by using the concept of the separation of source and field points.

By introducing the transforming matrix $[\mathbf{B}]$:

$$
[\mathbf{B}]_{2N\times 4} = [\mathbf{A}]^{-1}{}_{2N\times 2N}[\boldsymbol{\Phi}_{\mathbf{x}}]_{2N\times 4} \tag{41}
$$

to equation (37), we have:

$$
\begin{aligned}
[\mathbf{A}^{pt}]_{2N\times 2N}[\mathbf{B}]_{2N\times 4} &= [\boldsymbol{\Phi}_{\mathbf{x}}]_{2N\times 4} + \ln p[\boldsymbol{\Phi}_{\mathbf{x}}]_{2N\times 4}[\boldsymbol{\Psi}_{\mathbf{s}}]^T_{4\times 2N}[\mathbf{B}]_{2N\times 4} \\
&= [\boldsymbol{\Phi}_{\mathbf{x}}]_{2N\times 4}\left([\mathbf{I}]_{4\times 4} + \ln p[\boldsymbol{\Psi}_{\mathbf{s}}]^T_{4\times 2N}[\mathbf{B}]_{2N\times 4}\right)
\end{aligned}
\tag{42}
$$

where $[\boldsymbol{\Phi}_{\mathbf{X}}]_{2N\times 4}$ is the cofactor.

If the determinant of the matrix $[\mathbf{A}^{pt}]$ as:

$$
\left|[\mathbf{A}^{pt}]_{2N\times 2N}\right| = 0 \tag{43}
$$

it means:

$$
\left|[\mathbf{I}]_{4\times 4} + \ln p[\boldsymbol{\Psi}_{\mathbf{s}}]^T[\mathbf{B}]\right| = 0 \tag{44}
$$

By introducing equation (44), we can rearrange the linear algebraic system in equation (23) as:

$$\left([\mathbf{I}] + \ln p[\mathbf{\Psi_s}]^T[\mathbf{B}]\right)\{x\} = \{0\} \tag{45}$$

Equation (44) can be rewritten as:

$$\left([\mathbf{\Psi_s}]^T[\mathbf{B}] + \left(\frac{1}{\ln p}\right)[\mathbf{I}]\right)\{x\} = \{0\} \tag{46}$$

It is reformulated as a standard eigenproblem:

$$[\mathrm{K} - \lambda\,\mathrm{I}]\{x\} = \{0\} \tag{47}$$

where $\mathrm{K} = [\mathbf{\Psi_s}]^T[\mathrm{B}]$ and the scaling ratio is related to the eigenvalue as shown below:

$$p = e^{-1/\lambda} \tag{48}$$

The influence matrix of the biharmonic equation can be reduced to a 4 by 4 standard eigenproblem of equation (47). We can directly find the scaling ratio to obtain the degenerate scale.

3. Results and discussions

In this section, we apply two approaches to detect degenerate scales of three simple cases, a circle, an ellipse and a 30°–60°–90° triangle (as shown in Figure 3) of the biharmonic equation in the indirect BIE/BEM. The analytical results derived in the polar coordinates for a circular domain can be compared with the degenerate scale obtained from direct-searching scheme and scaling transform in the circular case.

3.1 Degenerate scales of a circle

First, we consider the problem of a circular domain. According to the above section, we analytically obtain degenerate scales ($R_d = e^{-1}$) by using the degenerate kernel. The scaling ratio to the ordinary-scale radius ($R_0 = 1$) is found as $p = \mathrm{e}^{-1} = 0.367879$. Therefore, the degenerate scale of a circular domain is 0.367879 (e^{-1}). The increments of the radius with the direct-searching scheme are 10^{-5}, 10^{-6} and 10^{-7} by using 80 constant elements (uniformly distributed). The results of the direct-searching scheme are shown in Figure 4. We can clearly find that the more accurate result is obtained by using the smaller increment of 10^{-7}. By meshing a large number of boundary elements,

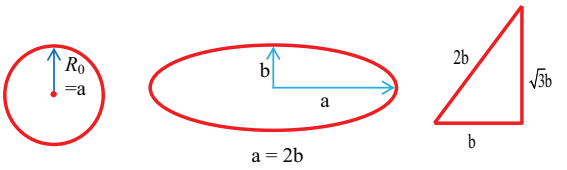

Figure 3.
Three cases of simple shapes for the biharmonic equation

Notes: (a) A circular domain; (b) an elliptic domain; (c) a right triangular domain (30°–60°–90°)

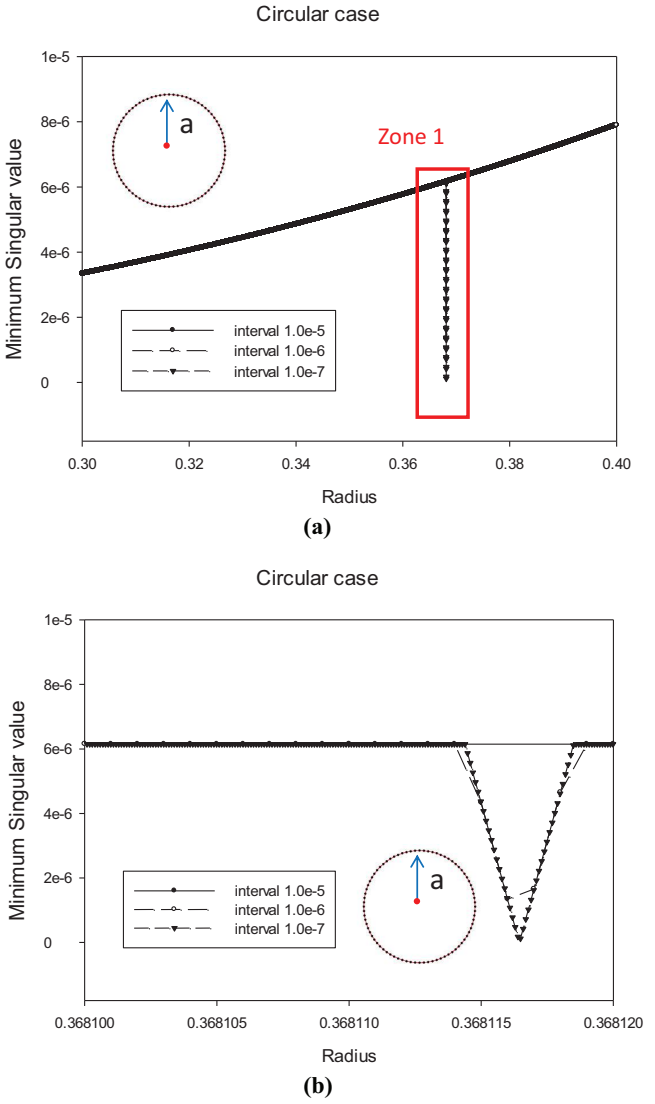

Notes: (a) Global view of the direct-searching scheme for a circular domain; (b) zone 1 of the direct-searching scheme for a circular domain

Figure 4.
The degenerate scale obtained versus different increments for a circular problem of the biharmonic equation in the indirect BEM by using the direct-searching scheme

we obtain the more accurate result in Figure 5. Eigenvalues for the circular domain by using the scaling transform and analytical derivation are shown in Table I. The comparison of the results for the degenerate scale by using three approaches, namely, analytical derivation, the direct-searching scheme and the 4 by 4 eigen system, is shown

in Table II. It is more efficient to obtain the acceptable result by using the scaling transform than by using the direct-searching scheme with the same number of elements. All the three approaches yield agreeable degenerate scales.

3.2 Degenerate scales of an ellipse

In the elliptical case, we consider the ratio of the length of the semi-minor axis b to the length of the semi-major axis a to be 0.5. By using the same increments of the circular case, we obtain the more acceptable result in the increment of 10^{-7} for the direct-searching scheme in Figure 6. Similarly, the larger the number of boundary elements is, the better results of two degenerate scales are obtained in Figure 7. Thanks to the scaling transform, we can obtain two different eigenvalues $\lambda_1 = 0.6363$ and $\lambda_2 = 0.8077$ for the scaling ratios, $p_1 = 0.2077$ and $p_2 = 0.2899$ for the length of the semi-major axis a in Table III, respectively. Therefore, the degenerate scales of an elliptical domain are

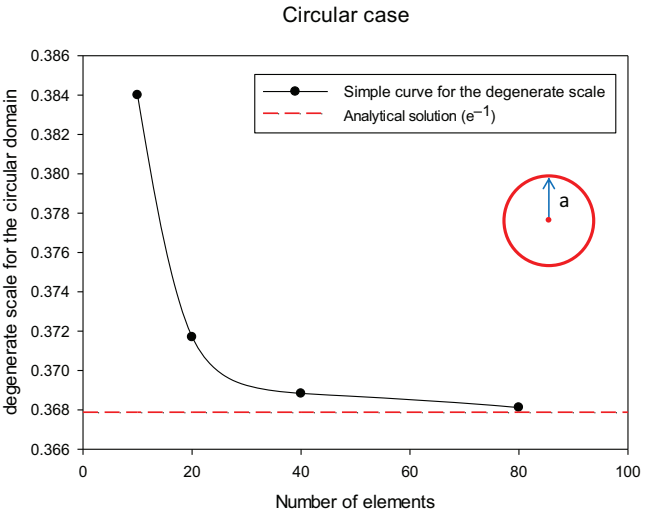

Figure 5.
Degenerate scale obtained versus different numbers of elements for a circular problem of the biharmonic equation in the indirect BEM by using the direct-searching scheme

Table I.
Eigenvalues for the circular plate by using the scaling transform and the analytical derivation

Numerical implementation for the scaling transform with 80 elements (λ)	Analytical solution (λ)
1.0006	1
1.0006	1
1.0003 + 1.0010i	1 + i
1.0003 − 1.0010i	1 − i

Table II.
Degenerate scales of the circular plate by using three approaches

Numerical implementation for the scaling transform with 80 elements	Analytical solution	Numerical implementation by using the direct-searching scheme with 80 elements
0.3681	0.3678	0.3681

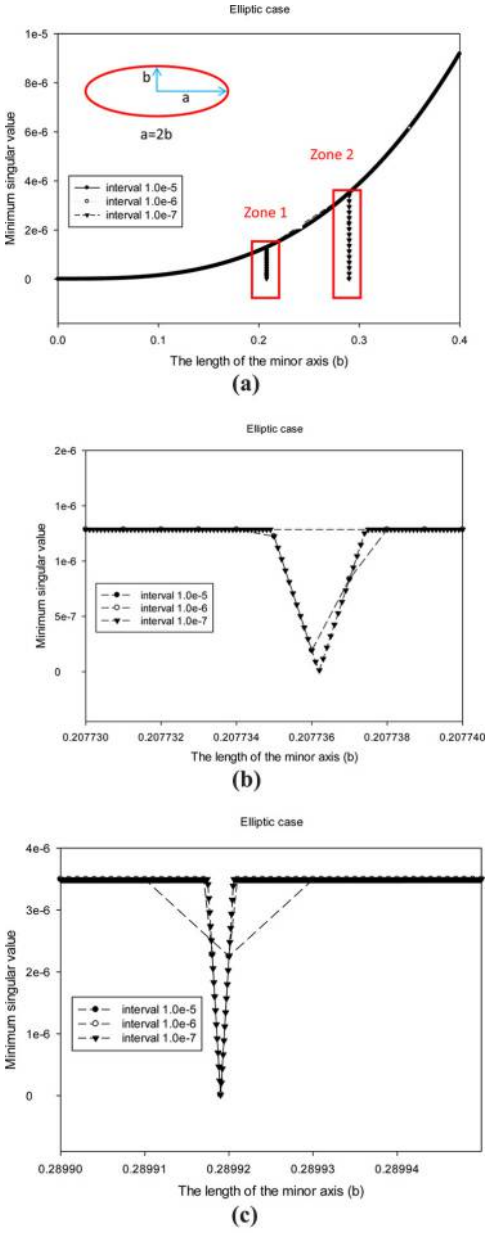

Notes: (a) Global view of the direct-searching scheme for an elliptic domain; (b) zone 1 of the direct-searching scheme for an elliptic domain; (c) zone 2 of the direct-searching scheme for an elliptic domain

Figure 6.
Two degenerate scales obtained versus different resolution for an elliptic problem of the biharmonic equation in the indirect BEM by using the direct searching scheme

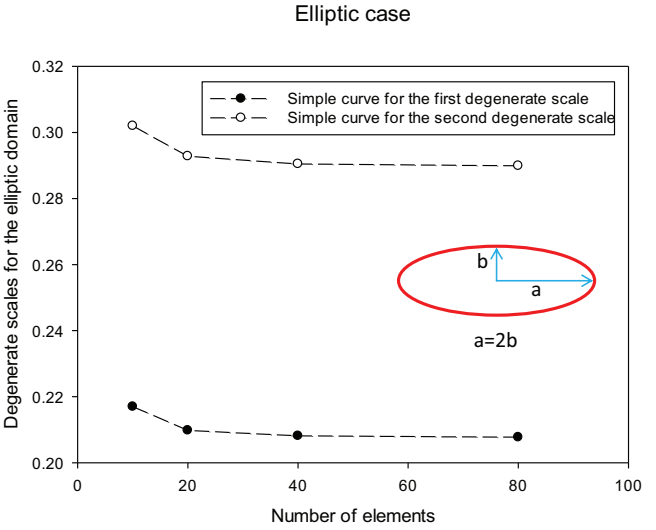

Figure 7.
Degenerate scales versus number of elements for an elliptic plate of the biharmonic equation in the indirect BEM by using the direct searching scheme

Table III.
Degenerate scales of the elliptic plate by using two approaches

Numerical implementation for the scaling transform with 80 elements	Numerical implementation by using the direct-searching scheme with 80 elements
0.2077 ($\lambda_1 = 0.6363$)	0.2077
0.2899 ($\lambda_2 = 0.8077$)	0.2899

0.2077 and 0.2899. It shows the validity of the scaling transform after comparing with the results of the direct-searching scheme in Table III.

3.3 Degenerate scales of a right triangle (30°–60°–90°)

In this case, we choose a special right triangle (30°–60°–90°) for the BEM by using 30 constant elements (10 elements for each side). The proportional ratio of lengths of a 30°–60°–90° triangle is $2:1:\sqrt{3}$. As lengths of three boundaries expand proportionally, we select the length of base of the right triangle as a reference. The two degenerate scales are obtained by using the direct-searching scheme in Figure 8. Based on the scaling transform, the two eigenvalues $\lambda_1 = 1.2384$ and $\lambda_2 = 2.5995$ are found. It means that two corresponding degenerate scales 0.4495 and 0.6836 are obtained in Table IV.

According to the results from the direct-searching scheme, the results may depend on the increment of size and pay effort for the small increment of high resolution. Degenerate scale obtained by using the direct-searching scheme may be different in one shape by taking various number of elements. It is an efficient way to obtain the degenerate scales immediately from the eigenvalues of a 4 by 4 matrix by using the scaling transform. By using the proposed method, the degenerate scale in radius, $R_d = 0.3681$, for Case 1 (circular case); degenerate scales in the minor length of the ellipse, $b_d = 0.2077$ and 0.2899, for Case 2 (elliptic case); and degenerate scales in base-side length of the right triangle, $b_d = 0.4495$ and 0.6836, for Case 3 (triangular case) were obtained.

4. Relation of degenerate scales and the fundamental solution

According to the experience of previous examples, we find complex eigenvalues which are not geometrically realizable. To explain this phenomenon, we theoretically demonstrate that degenerate scales depend on the kernel function. By adding a free constant, all real degenerate scales may be obtained and are elaborated on later. To transform the roots of original eigen system to be all real, we can add a constant to the fundamental solution. It can be represented from equation (8) as:

$$U(\mathbf{x},\mathbf{s})=r^2\ln R+c$$

$$=\begin{cases} U^I(\mathbf{x},\mathbf{s})=c+\rho^2(1+\ln R)+R^2\ln R-\left[R\rho(1+2\ln R)+\frac{1}{2}\frac{\rho^3}{R}\right]\cos(\theta-\phi) \\ -\sum_{m=2}^{\infty}\left[\frac{1}{m(m+1)}\frac{\rho^{m+2}}{R^m}-\frac{1}{m(m-1)}\frac{\rho^m}{R^{m-2}}\right]\cos[m(\theta-\phi)], \quad R\geq\rho, \\ U^E(\mathbf{x},\mathbf{s})=c+R^2(1+\ln\rho)+\rho^2\ln\rho-\left[\rho R(1+2\ln\rho)+\frac{1}{2}\frac{R^3}{\rho}\right]\cos(\theta-\phi) \\ -\sum_{m=2}^{\infty}\left[\frac{1}{m(m+1)}\frac{R^{m+2}}{\rho^m}-\frac{1}{m(m-1)}\frac{R^m}{\rho^{m-2}}\right]\cos[m(\theta-\phi)], \quad \rho>R \end{cases} \tag{49}$$

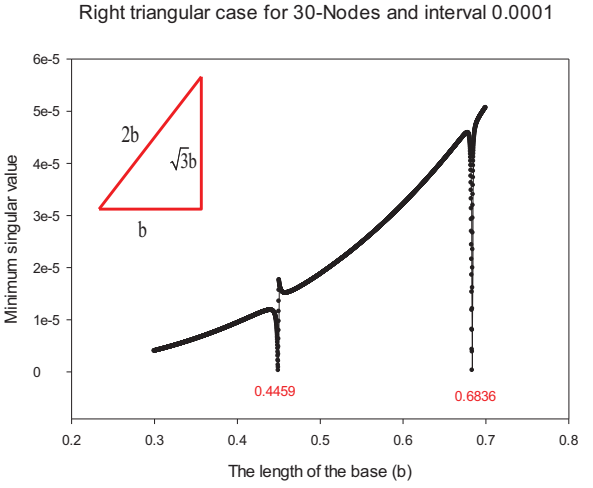

Figure 8. Degenerate scales obtained versus different resolution for a non-right-isosceles triangular problem of the biharmonic equation in the indirect BEM by using the direct searching scheme

Table IV. Degenerate scales of the right triangular plate (30°–60°–90°) by using two approaches

Numerical implementation for the scaling transform with 30 elements	Numerical implementation by using the direct-searching scheme with 30 elements
0.4495 ($\lambda_1 = 1.2384$)	0.4495
0.6836 ($\lambda_2 = 2.5995$)	0.6836

and equation (14) can be rewritten as:

$$\int_B U(\mathbf{s},\mathbf{x})\alpha(\mathbf{s})dB(\mathbf{s}) = 2c\pi R_0 a_0 + 2\pi(1+2\ln R_0)R_0^3 a_0 - \pi\left(\frac{3}{2}+2\ln R_0\right)a_1 R_0^3\cos\phi$$
$$-\pi\left(\frac{3}{2}+\ln R_0\right)b_1 R_0^3\sin\phi + \sum_{m=2}^{\infty}\frac{2\pi}{m(m+1)(m-1)}a_m R_0^3\cos m\phi$$
$$+\sum_{m=2}^{\infty}\frac{2\pi}{m(m+1)(m-1)}b_m R_0^3\sin m\phi = 2\pi\left(\frac{c}{R_0^2}+1+2\ln R_0\right)R_0^3 a_0$$
$$-\pi\left(\frac{3}{2}+2\ln R_0\right)a_1 R_0^3\cos\phi - \pi\left(\frac{3}{2}+\ln R_0\right)b_1 R_0^3\sin\phi$$
$$+\sum_{m=2}^{\infty}\frac{2\pi}{m(m+1)(m-1)}a_m R_0^3\cos m\phi + \sum_{m=2}^{\infty}\frac{2\pi}{m(m+1)(m-1)}b_m R_0^3\sin m\phi \tag{50}$$

As c is a constant, the other parts of the influence matrix [the normal derivatives of equation (50)] remain the same as equations (15)-(17). By comparing the coefficient and taking three terms (the constant term, the term related to cos θ and the term related to sin θ), the coefficient can be formed as:

$$\begin{bmatrix}
2\pi\left(\frac{c}{R_0^2}+1+2\ln R_0\right)R_0^3 & 4\pi(1+\ln R_0)R_0^2 & 0 & 0 & 0 & 0\\
4\pi(1+\ln R_0)R_0^2 & 4\pi R_0 & 0 & 0 & 0 & 0\\
0 & 0 & -\pi\left(\frac{3}{2}+2\ln R_0\right)R_0^3 & -\pi\left(\frac{5}{2}+2\ln R_0\right)R_0^2 & 0 & 0\\
0 & 0 & -\pi\left(\frac{5}{2}+2\ln R_0\right)R_0^2 & -\pi\left(\frac{3}{2}+2\ln R_0\right)R_0 & 0 & 0\\
0 & 0 & 0 & 0 & -\pi\left(\frac{3}{2}+2\ln R_0\right)R_0^3 & -\pi\left(\frac{5}{2}+2\ln R_0\right)R_0^2\\
0 & 0 & 0 & 0 & -\pi\left(\frac{5}{2}+2\ln R_0\right)R_0^2 & -\pi\left(\frac{3}{2}+2\ln R_0\right)R_0
\end{bmatrix}
\begin{Bmatrix} a_0^c\\ c_0^c\\ a_1^c\\ c_1^c\\ b_1^c\\ d_1^c \end{Bmatrix} = \begin{Bmatrix} e_0\\ g_0\\ e_1\\ f_1\\ g_1\\ h_1 \end{Bmatrix} \tag{51}$$

The submatrix of the constant term is singular due to the zero determinant:

$$8\pi^2\left(\frac{c}{R_d^2}+1+2\ln R_d\right)R_d^4 - 16\pi^2(1+\ln R_d)^2 R_d^4 = 0 \tag{52}$$

It means that extra degenerate scales occur while the adding constant is

$$c = R_d^2\left(2(\ln R_d)^2 + 2\ln R_d + 1\right) \tag{53}$$

in Figure 9. If the degenerate scale $R_d = e^{-1}$, the corresponding constant $c = e^{-2}$ obtained from equation (53) for the constant term of equation (51). The determinant of

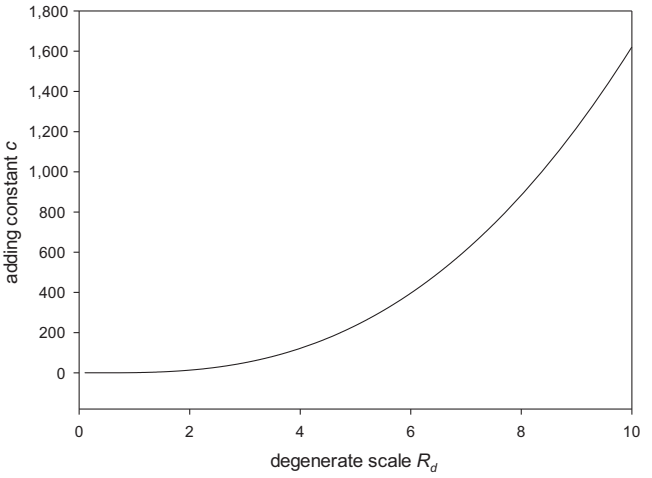

Figure 9.
Relationship between the adding constant c and the degenerate scale R_d

the submatrix from the term related to cos θ or the term related to sin θ in equation (51) is the same as equation (22), and we can find the degenerate scale $R_d = e^{-1}$. It means that four real scales exist (e^{-1}, multiplicity = 4) while we consider the fundamental solution of equation (49). Therefore, a degenerate scale depends on the kernel function. Although we have four eigenvalues, two real roots (realizable) and two complex roots (unrealizable) in our case of $U(\mathbf{x}, \mathbf{s}) = r^2 \ln r$, we can have a root of multiplicity 4 by adding a constant to the fundamental solution as $U(\mathbf{x}, \mathbf{s}) = r^2 \ln r + c$. Table V summarizes the influence matrices and degenerate scales after adding a constant for a rod, a beam, a circular membrane and a circular plate.

5. Conclusions

By using the degenerate kernel and Fourier expansion in the polar coordinates, the analytical degenerate scale of the circular biharmonic equation can be derived. The extra matrix $[\mathbf{A}^s]$ due to scaling for the biharmonic equation can be decomposed into two matrices related to the source and field points separately. By using the scaling transform, the $2N$ by $2N$ influence matrix of the biharmonic equation can be reduced to a 4 by 4 eigenproblem for all shapes in the numerical implementation. The results of analytical derivation, the direct-searching method and the 4 by 4 eigenproblem are acceptable in searching degenerate scales of the 2D biharmonic equation. A 4 by 4 eigenproblem to search degenerate scales is more efficient than the direct-searching method. However, the result of 2 real and 2 complex eigenvalues by using the fundamental solution can be changed to 4 real eigenvalues through adding the constant c into the fundamental solution. It means that the extra degenerate scales (or rank deficiency) depend on the kernel function. Finally, several cases show acceptable results. The proposed method can be applied in searching the degenerate scales analytically, semi-analytically by using the 4 by 4 eigen system and numerically by using the direct-searching scheme.

Table V.
The influence matrices and degenerate scales for a rod, a beam, a circular membrane and a circular plate

	The fundamental solution	Influence matrix[A]	Degenerate scale	Reference
1D rod	$U(\mathrm{s},\mathrm{x}) = \frac{1}{2}\lvert\mathrm{x}-\mathrm{s}\rvert + a\mathrm{s} + c$	$\frac{EA}{l}\begin{bmatrix} 1 & -1 \\ -1 & 1 \end{bmatrix}$	$(1+2a)l = -4c$	Chen *et al.* (2003b)
1D beam	$U(\mathrm{s},\mathrm{x}) = \frac{1}{12}\lvert\mathrm{x}-\mathrm{s}\rvert^3 + a\mathrm{s} + b\mathrm{s}^2 + d\mathrm{s}^3 + c$	$\frac{EA}{l^3}\begin{bmatrix} 12 & 6l & -12 & 6l \\ 6l & 4l^2 & 6l & 2l^2 \\ -12 & -6l & 12 & -6l \\ 6l & 2l^2 & -6l & 4l^2 \end{bmatrix}$	$(1+12d)l^3 - 24al = 48c$	
2D circular membrane	$U(\mathrm{s},\mathrm{x}) = \ln r + pR\cos(\theta) + qR\sin(\theta) + c$	$\begin{bmatrix} 0 & 0 & \cdots & \cdots & 0 \\ 0 & \frac{1}{R} & 0 & \cdots & \cdots \\ \vdots & 0 & \ddots & 0 & \vdots \\ \vdots & \vdots & 0 & \frac{N-1}{R} & 0 \\ 0 & 0 & \cdots & 0 & \frac{N}{R} \end{bmatrix}$	$\ln R_d = -c$	
2D circular plate	$U(\mathrm{s},\mathrm{x}) = r^2 \ln r + c$	$\begin{bmatrix} [\mathbf{U}] & [\boldsymbol{\Theta}] \\ [\mathbf{U}_\theta] & [\boldsymbol{\Theta}_\theta] \end{bmatrix}$	$R_d = e^{-1}$ and $c = R_d^2\left(2(\ln R_d)^2 + 2\ln R_d + 1\right)$	Present method

References

Chen, G. and Zhou, J. (1992), *Boundary Element Methods*, Academic Press, New York, NY.

Chen, Y.Z. and Lin, X.Y. (2010), "Dual boundary integral equation formulation in antiplane elasticity using complex variable", *Computational Mechanics*, Vol. 45 No. 2, pp. 167-178.

Chen, Y.Z. and Wang, Z.X. (2015), "Properties of integral operators and solutions for complex variable boundary integral equation in plane elasticity for multiply connected regions", *Engineering Analysis with Boundary Elements*, Vol. 52, pp. 44-55.

Chen, J.T., Lin, S.R. and Chen, K.H. (2005a), "Degenerate scale problem when solving Laplace equation by BEM and its treatment", *International Journal for Numerical Methods in Engineering*, Vol. 62 No. 2, pp. 233-261.

Chen, J.T., Hsiao, C.C. and Leu, S.Y. (2007b), "A new method for Stokes' flow with circular boundaries using degenerate kernel and Fourier series", *International Journal for Numerical Methods in Engineering*, Vol. 74, pp. 1955-1987.

Chen, J.T., Liao, H.Z. and Lee, W.M. (2009d), "An analytical approach for the green's functions of biharmonic problems with circular and annular domains", *Journal of Mechanics*, Vol. 25 No. 1, pp. 59-74.

Chen, Y.Z., Lin, X.Y. and Wang, Z.X. (2009b), "Evaluation of the degenerate scale for BIE in plane elasticity and antiplane elasticity by using conformal mapping", *Engineering Analysis with Boundary Elements*, Vol. 33 No. 2, pp. 147-159.

Chen, Y.Z., Lin, X.Y. and Wang, Z.X. (2009c), "Numerical solution for degenerate scale problem for exterior multiply connected region", *Engineering Analysis with Boundary Elements*, Vol. 33 No. 11, pp. 1316-1321.

Chen, Y.Z., Wang, Z.X. and Lin, X.Y. (2009a), "The degenerate scale problem for the Laplace equation and plane elasticity in a multiply connected region with an outer circular boundary", *International Journal of Solids and Structures*, Vol. 46 No. 13, pp. 2605-2610.

Chen, J.T., Wu, C.S. and Chen, K.H. (2005b), "A study of free terms for plate problems in the dual boundary integral equations", *Engineering Analysis with Boundary Elements*, Vol. 29 No. 5, pp. 435-446.

Chen, J.T., Chen, K.H., Chen, I.L. and Liu, L.W. (2003a), "A new concept of modal participation factor for numerical instability in the dual BEM for exterior acoustics", *Mechanics Research Communications*, Vol. 30 No. 6, pp. 161-174.

Chen, J.T., Chen, W.C., Lin, S.R. and Chen, I.L. (2003b), "Rigid body mode and spurious mode in the dual boundary element formulation for the Laplace equation", *Computers and Structures*, Vol. 81 No. 13, pp. 1395-1404.

Chen, J.T., Han, H.D., Kuo, S.R. and Kao, S.K. (2014), "Regularized methods for ill-conditioned system of the integral equations of the first kind", *Inverse Problems in Science and Engineering*, Vol. 22 No. 7, pp. 1176-1195.

Chen, J.T., Kuo, S.R., Kao, S.K. and Jian, J. (2015), "Revisit of a degenerate scale: a semi-circular disk", *Journal of Computational Applied Mathematics*, Vol. 283, pp. 182-200.

Chen, J.T., Lin, J.H., Kuo, S.R. and Chiu, Y.P. (2001), "Analytical study and numerical experiments for degenerate scale problems in boundary element method using degenerate kernels and circulants", *Engineering Analysis with Boundary Elements*, Vol. 25 No. 9, pp. 819-828.

Chen, J.T., Lee, C.F., Chen, I.L. and Lin, J.H. (2002), "An alternative method for degenerate scale problems in boundary element methods for the two-dimensional Laplace equation", *Engineering Analysis with Boundary Elements*, Vol. 26 No. 7, pp. 559-569.

Chen, J.T., Lee, Y.T., Chang, Y.L. and Jian, J. (2017a), "A self-regularized approach for rank-deficiency systems in the BEM of 2D Laplace problems", *Inverse Problems in Science and Engineering*, Vol. 25 No. 1, pp. 89-113.

Chen, J.T., Lee, Y.T., Kuo, S.R. and Chen, Y.W. (2012), "Analytical derivation and numerical experiments of degenerate scale for an ellipse in BEM", *Engineering Analysis with Boundary Elements*, Vol. 36 No. 9, pp. 1397-1405.

Chen, J.T., Wu, C.S., Chen, K.H. and Lee, Y.T. (2006a), "Degenerate scale for analysis of circular plate using the boundary integral equations and boundary element method", *Computational Mechanics*, Vol. 38, pp. 33-49.

Chen, J.T., Wu, C.S., Lee, Y.T. and Chen, K.H. (2007a), "On the equivalence of the Trefftz method and method of fundamental solutions for Laplace and biharmonic equations", *Computers and Mathematics with Applications*, Vol. 53 No. 6, pp. 851-879.

Chen, J.T., Huang, W.S., Lee, Y.T., Kuo, S.R. and Kao, S.K. (2017b), "Revisit of degenerate scales in the BIEM/BEM for 2D elasticity problems", *Mechanics of Advanced Materials and Structures*, Vol. 24 No. 1, pp. 1-15.

Christiansen, S. (2001), "Detecting non-uniqueness of solutions to biharmonic integral equations through SVD", *Journal of Computational Applied Mathematics*, Vol. 134, pp. 23-35.

Constanda, C. (1993), "On the solution of the Dirichlet problem for the two dimensional Laplace equation", *Proceedings of the American Mathematical Society*, Vol. 119, pp. 877-884.

Constanda, C. (1997), "On the Dirichlet problem for the two dimensional biharmonic equation", *Mathematical Methods in the Applied Sciences*, Vol. 20, pp. 885-890.

Corfdir, A. and Bonnet, G. (2013), "Degenerate scale for the Laplace problem in the half-plane; approximate logarithmic capacity for two distant boundaries", *Engineering Analysis with Boundary Elements*, Vol. 37, pp. 836-841.

Corfdir, A. and Bonnet, G. (2016), "Exact degenerate scales in plane elasticity using complex variable methods", *International Journal of Solids and Structures*, Vol. 80, pp. 430-444.

Costabel, M. and Dauge, M. (1996), "Invertibility of the biharmonic single layer potential operator", *Integral Equations and Operator Theory*, Vol. 24 No. 1, pp. 46-67. No

Dijkstra, W. and Mattheij, R.M.M. (2007), "A relation between the logarithmic capacity and the condition number of the BEM-matrices", *Communications in Numerical Methods in Engineering*, Vol. 23 No. 7, pp. 665-680.

Fadhil, S. and El-Zafrany, A. (1994), "Boundary element analysis of thick Reissner plates on two-parameter foundation", *International Journal of Solids and Structures*, Vol. 31 No. 21, pp. 2901-2917.

Han, H.D., Lee, Y.T., Yin, D.S. and Chen, J.T. (2015), "The necessary and sufficient condition for the existence and uniqueness of a system of Fredholm integral equations of the first kind", *Scientia Sinina Mathmatica*, Vol. 45 No. 8, pp. 1231-1248 (in Chinese).

Hayes, J. and Kellner, R. (1972), "The eigenvalue problem for a pair of coupled integral equations arising in the numerical solution of Laplace equation", *SIAM Journal on Applied Mathematics*, Vol. 22 No. 3, pp. 503-513.

He, W.J. (2000), "An equivalent boundary integral formulation for bending problems of thin plates", *Computers and Structures*, Vol. 74, pp. 319-322.

He, W.J., Ding, H.J. and Hu, H.C. (1996), "Non-equivalence of the conventional boundary integral formulation and its elimination for two-dimensional mixed potential problems", computers and structures", Vol. 60, pp. 1029-1035.

Hille, E. (1962), *Analytical Function Theory*, Ginn Comp, Boston, MA, Vol. 2.

Jaswon, M.A. and Maiti, M. (1968), "An integral equation formulation of plate bending problems", *Journal of Engineering Mathematics*, Vol. 2 No. 1, pp. 83-93.

Jaswon, M.A., Maiti, M. and Symm, G.T. (1967), "Numerical biharmonic analysis and some applications", *International Journal of Solids and Structures*, Vol. 3 No. 3, pp. 309-332.

Kuo, S.R., Chen, J.T. and Kao, S.K. (2013a), "Linkage between the unit logarithmic capacity in the theory of complex variables and the degenerate scale in the BEM/BIEMs", *Applied Mathematics Letters*, Vol. 29 No. 6, pp. 929-938.

Kuo, S.R., Chen, J.T., Lee, J.W. and Chen, Y.W. (2013b), "Analytical derivation and numerical experiments of degenerate scale for regular N-gon domains in BEM", *Applied Mathematics and Computation*, Vol. 219, pp. 5668-5683.

Lee, M.G., Li, Z.C., Huang, H.T. and Chiang, J.Y. (2013), "Conservative schemes and degenerate scale problems in the null-field method for Dirichlet problems of Laplace's equation in circular domains with circular holes", *Engineering Analysis with Boundary Elements*, Vol. 37, pp. 95-106.

Manolis, G.D., Rangelov, T.V. and Shaw, R.P. (2003), "The non-homogeneous biharmonic plate equation: fundamental solutions", *International Journal of Solids and Structures*, Vol. 40 No. 21, pp. 5753-5767.

Mitra, A.K. and Das, S. (1988), "Nonuniqueness in the integral equations formulation of the biharmonic equation in multiply connected domains", *Computer Methods in Applied Mechanics and Engineering*, Vol. 69, pp. 205-214.

Petrovsky, I.G. (1954), *Lectures on Partial Differential Equations (A. Shenitzer, Trans.)*, Interscience, New York, NY.

Stern, M. (1979), "A general boundary integral formulation for the numerical solution of plate bending problems", *International Journal of Solids and Structures*, Vol. 15 No. 10, pp. 769-782.

Tsiatas, G.C. (2009), "A new Kirchhoff plate model based on a modified couple stress theory", *International Journal of Solids and Structures*, Vol. 46 No. 13, pp. 2757-2764.

Vodička, R. and Mantič, V. (2004), "On invertibility of elastic singlelayer potential operator", *Journal of Elasticity*, Vol. 74, pp. 147-173.

Vodička, R. and Mantič, V. (2008), "On solvability of a boundary integral equation of the first kind for Dirichlet boundary value problems in plane elasticity", *Computational Mechanics*, Vol. 41 No. 6, pp. 817-826. No

Yan, Y. and Sloan, I.H. (1988), "On integral equations of the first kind with logarithmic kernels", *Journal of Integral Equations and Applications*, Vol. 1, pp. 549-580.

Yu, D.H. (1982), "Canonical integral equations of bi-harmonic elliptic boundary value problems", *Mathematica Numerica Sinica*, Vol. 4 No. 3, pp. 330-336.

Yu, D.H. (1983), "Numerical solutions of harmonic and biharmonic canonical integral equations in interior or exterior circular domains", *Journal of Computational Mathematics*, Vol. 1 No. 1, pp. 52-62.

Yu, D.H. (1993), *Mathematical Theory of Natural Boundary Element Method*, Science Press, Beijing.

Yu, D.H. (2002), *The Natural Boundary Integral Method and Its Applications*, Science Press & Kluwer Academic Publishers.

Zhou, S.J., Sun, S.X. and Cao, X.Y. (1999), "The boundary contour method based on the equivalent boundary integral equation for 2-D linear elasticity", *Communications in Numerical Methods in Engineering*, Vol. 15 No. 11, pp. 811-821.

Further reading

Chen, J.T., Chen, K.H., Yeih, W. and Shieh, N.C. (1998), "Dual boundary element analysis for cracked bars under torsion", *Engineering Computations*, Vol. 15 No. 6, pp. 732-749.

Chen, J.T., Hsziao, C.C. and Leu, S.Y. (2006b), "Null-field integral equation approach for plate problems with circular boundaries", *Journal of Applied Mechanics*, Vol. 73 No. 4, pp. 679-693.

About the authors

Jeng-Tzong Chen is a Professor in the Department of Harbor and River Engineering and Department of Mechanical and Mechatronic Engineering, National Taiwan Ocean University, Keelung, Taiwan. He is also the vice president of TwSIAM (Taiwan Society for Industrial and Applied Mathematics) and associated editor of *Journal of Mechanics* and *Journal of Chinese Institute of Engineers*. Jeng-Tzong Chen is the corresponding author and can be contacted at: jtchen@mail.ntou.edu.tw

Shyh-Rong Kuo is a Professor in the Department of Harbor and River Engineering, National Taiwan Ocean University, Keelung, Taiwan.

Yu-Lung Chang is a Post Doctor in the Department of Harbor and River Engineering, National Taiwan Ocean University, Keelung, Taiwan.

Shing-Kai Kao is a Research Assistant in the Department of Harbor and River Engineering, National Taiwan Ocean University, Keelung, Taiwan.